7LAMINAR CONVECTIVE HEAT TRANSFER FOR IN-PLANE SPIRAL COILS OF NON-CIRCULAR CROSS-SECTIONS DUCTS
A Computational Fluid Dynamics Study

by

Jundika C. KURNIA [a], *Agus P. SASMITO* [b], *and Arun S. MUJUMDAR* [a, c*]

[a] Department of Mechanical Engineering, National University of Singapore, Singapore
[b] Mechanical Engineering, Masdar Institute of Science and Technology, Abu Dhabi, United Arab Emirates
[b] Mineral, Metal and Material Technology Centre, National University of Singapore, Singapore

The objective of this study was to carry out a parametric study of laminar flow and heat transfer characteristics of coils made of tubes of several different cross--sections e. g. square, rectangular, half-circle, triangular, and trapezoidal. For the purpose of ease of comparison, numerical experiments were carried out base on a square-tube Reynolds number of 1000 and a fixed fluid flow rate while length of the tube used to make coils of different diameter and pitch was held constant. A figure of merit was defined to compare the heat transfer performance of different geometry coils; essentially it is defined as total heat transferred from the wall to the surroundings per unit pumping power required. Simulations were carried out for the case of constant wall temperature as well as constant heat flux. In order to allow reasonable comparison between the two different boundary conditions – constant wall temperature and constant wall heat flux – are tested; the uniform heat flux boundary condition was computed by averaging the heat transferred per unit area of the tube for the corresponding constant wall temperature case. Results are presented and discussed in the light of the geometric effects which have a significant effect on heat transfer performance of coils.

Key words: *coil, non-circular tube, heat transfer performance, mathematical model*

Introduction

First introduced in 19th century [1], in-plane spiral tubes have been widely implemented in engineering application due to their higher heat transfer performance, compact structure, and ease of manufacture. They are commonly used in heat exchanger, electronic cooling, chromatography, fuel cell coolant channel, chemical reactor, and many others applications. Transport phenomena occurring in spiral tubes are more complicated than those in straight ducts. The reason for this is the presence of secondary flows due to centrifugal forces that significantly affect heat and mass transport. As such, spiral tubes have

---

* Corresponding author; e-mail: mpeasm@nus.edu.sg

also attracted attention from engineering researchers even though they are less popular compared to helical tubes, which have attracted major attention in the study of coiled tubes for heat transfer.

Dean [2, 3] was among first researchers who studied fluid flow inside a toroidal (in-plane) constant radius duct. This study revealed that circular tubes develop a secondary flow when the Dean number exceeds a critical value. Since then several experimental [4-10] and numerical [11-16] studies have been conducted in attempts to examine the transport phenomena in the spiral tubes. Most of these studies deal with spiral ducts with the typical cross-sections being circular or rectangular.

This paper addresses heat transfer performance of in-plane spiral ducts of various cross-sections, *e. g.* square, rectangular, half-circle, triangular, and trapezoidal, with the aim to determine optimum design of in-plane spiral duct for heat transfer application. A mathematical model for laminar flow of a Newtonian fluid in helical coils with square cross-section is developed. Two common thermal boundary conditions – constant wall temperature and constant heat flux – were simulated. The effect of Prandtl number was investigated by conducting simulations for air and water.

Computational fluid dynamics simulations were conducted for a square-duct Reynolds number of 1000 and a fixed fluid flow rate while length of the duct used to make coils of different diameter and pitch was also held constant. To compare the heat transfer performance of different geometry coils, a figure of merits (F_{merit}) is defined. It is the ratio of heat transferred from the wall to the fluid per unit pumping power supplied. Results are presented and discussed in the light of the geometric effects which were found to have a significant effect on the heat transfer performance of coils.

Mathematical model

Governing equations

Here incompressible laminar Newtonian fluid flows inside an in-plane spiral duct with various cross-sections are considered. The configurations of in-plane spiral ducts and their cross-section schematic are presented in fig. 1 and details of the geometric properties are summarized in tab. 1. Both constant wall heat flux and constant wall temperature conditions were investigated.

Since this work relates only to laminar flow, a precise numerical solution is adequate to simulate reality very closely. Conservation equations for mass, momentum and energy for the flow inside the ducts are given by:
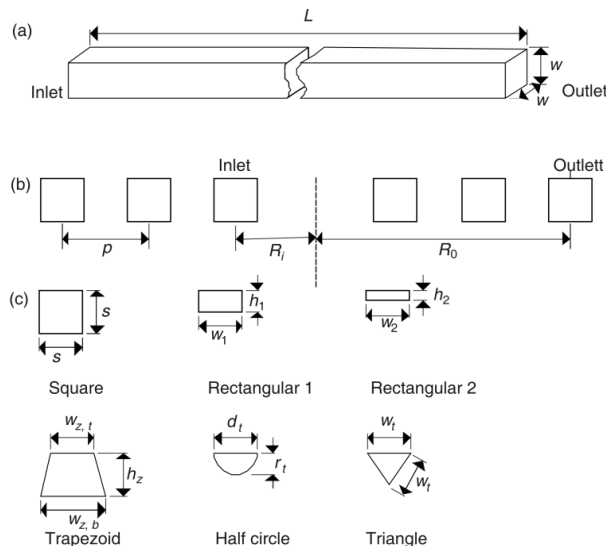

Figure 1. Schematic representation of (a) straight duct, (b) in-plane spiral duct, and (c) various cross-sections of in-plane spiral ducts

Kurnia, J. C., *et al.*: Laminar Convective Heat Transfer for In-Plane Spiral Coils of …
THERMAL SCIENCE, Year 2012, Vol. 16, No. 1, pp. 109-118

111

$$\nabla \rho \vec{u} = 0 \qquad (1)$$

$$\nabla (\rho \vec{u} \times \vec{u}) = -\nabla P + \nabla \mu \{ \nabla \vec{u} + (\nabla \vec{u})^T \} \quad (2)$$

$$\rho c_p \vec{u} \nabla T = k \nabla^2 T \qquad (3)$$

where ρ is the fluid density, $\vec{u}$ – the fluid velocity, P – the pressure, μ – the dynamic viscosity of the fluid, c_p – the specific heat of the fluid, k – the thermal conductivity, and T – the temperature.

Table 1. Geometric parameters used in simulations

Parameters	Value	Unit	Parameters	Value	Unit
L	1.2	m	$w_{z,b}$	$1.5 \cdot 10^{-2}$	m
w	$1 \cdot 10^{-2}$	m	h_z	$1 \cdot 10^{-2}$	m
s	$1 \cdot 10^{-2}$	m	d_t	$1 \cdot 10^{-2}$	m
w_1	$1 \cdot 10^{-2}$	m	r_t	$5 \cdot 10^{-3}$	m
h_1	$5 \cdot 10^{-3}$	m	w_t	$1 \cdot 10^{-2}$	m
w_2	$1 \cdot 10^{-2}$	m	R_i	$2 \cdot 10^{-2}$	m
h_2	$2.5 \cdot 10^{-3}$	m	R_0	$9 \cdot 10^{-2}$	m
$w_{z,t}$	$1 \cdot 10^{-2}$	m	p	$2 \cdot 10^{-2}$	m

Constitutive relations

Two working fluids are modeled to investigate the effect of Prandtl number, air and water. Thermophysical properties of these fluids are treated as temperature-dependent.

Air properties were obtained as polynomial functions of temperature [17]; the air density is defined by:

$$\rho_{air} = 1.076 \cdot 10^{-5} T^2 - 1.039 \cdot 10^{-2} T + 3.326 \qquad (4)$$

while the air viscosity is given by:

$$\mu_{air} = 5.21 \cdot 10^{-15} T^3 - 4.077 \cdot 10^{-11} T^2 + 7.039 \cdot 10^{-8} T + 9.19 \cdot 10^{-7} \qquad (5)$$

the thermal conductivity of air is calculated from:

$$k_{air} = 4.084 \cdot 10^{-10} T_{air}^3 - 4.519 \cdot 10^{-7} T_{air}^2 + 2.35 \cdot 10^{-4} T_{air} - 0.0147 \qquad (6)$$

and the specific heat of air is defined as:

$$c_{p,air} = -4.647 \cdot 10^{-6} T^3 + 4.837 \cdot 10^{-3} T^2 - 1.599 T + 1175 \qquad (7)$$

The density, viscosity, thermal conductivity, and specific heat of water are described as [11]:

$$\rho_w = -3.570 \cdot 10^{-3} T^2 + 1.88 T + 753.2 \qquad (8)$$

$$\mu_w = 2.591 \cdot 10^{-5} \cdot 10^{\frac{238.3}{T - 143.2}} \qquad (9)$$

$$k_w = -8.354 \cdot 10^{-6} T^2 + 6.53 \cdot 10^{-3} T - 0.5981 \qquad (10)$$

$$c_{p,w} = 4200 \qquad (11)$$

The results will be discussed later in terms of the mixed mean temperature variation along the ducts, total heat rate and figure of merit. The mixed mean temperature is given by [17]:

$$T_{\text{mean}} = \frac{1}{VA_c} \int_{A_c} T\vec{u}dA_c \qquad (12)$$

where V is the mean velocity given by [11]:

$$V = \frac{1}{A_c} \int_{A_c} \vec{u}dA_c \qquad (13)$$

The total heat rate and figure of merit, F_{merit}, are defined by:

$$\dot{Q}_{\text{total}} = \dot{m}c_p(T_{\text{mean, L}} - T_{\text{mean,0}}) \qquad (14)$$

$$F_{\text{merit}} = \frac{\dot{Q}_{\text{total}}}{\Delta P} \qquad (15)$$

Boundary conditions

The boundary conditions for the fluid flow inside ducts are defined as:

− inlet

$$\dot{m}_{\text{in}} = \dot{m}_{\text{in}}, \quad T = T_{\text{in}} \qquad (16)$$

− outylet

$$P = P_{\text{out}}, \vec{n}(\vec{e}_x, \vec{e}_y, \vec{e}_z)(k\nabla T) = 0 \qquad (17)$$

− wall

$$\vec{u} = 0, \ T = T_{\text{w}} \ \text{or} \ \vec{n}(\vec{e}_x, \vec{e}_y, \vec{e}_z)(k\nabla T) = Q_{\text{w}} \qquad (18)$$

The values for these variables are summarized in tab. 1.

Description of numerical approach

The computational domains (see fig. 2) were created in the AutoCAD 2010 software; the commercial pre-processor software GAMBIT 2.3.16 was used for meshing, labeling boundary conditions and determines the computational domain. After mesh independence test, the computational domain was resolved with around $2\cdot10^5$ to $4\cdot10^5$ elements: a fine structured mesh near the wall to resolve the boundary layer and an increasingly coarser mesh in the middle of the channel in order to reduce the computational cost.

The mathematical model given by eqs. (1)-(3) together with appropriate boundary condition and constitutive relations comprising five dependent variables: u, v, w, P, and T – was then solved by using commercial finite volume solver Fluent 6.3.26 and user-defined functions (UDF) written in C language to allow temperature-dependence of the thermophysical properties of the fluid.

Kurnia, J. C., *et al.*: Laminar Convective Heat Transfer for In-Plane Spiral Coils of …
THERMAL SCIENCE, Year 2012, Vol. 16, No. 1, pp. 109-118

113

The model was solved with the well-known semi-implicit pressure-linked equation (SIMPLE) algorithm, first-order upwind discretization and algebraic multi-grid (AMG) method. As an indication of the computational cost, it is noted that on average, around 200-500 iterations are needed for convergence criteria for all relative residuals of 10^{-6}; this takes 5-15 minutes on a workstation with a quad-core processor (1.8 GHz) and 8 GB of RAM.

Results and discussion

The numerical simulations were carried out for a square-duct Reynolds number of 1000 and a fixed fluid flow rate. Details parameter used for these simulations are presented in tab. 2.

This study examined seven different non-circular duct geometries: straight duct, in-plane spiral ducts with various cross-section geometries including square, 2×1 and 4×1 rectangular, trapezoid, triangular, and half-circular. Earlier investigations have shown that the presence of centrifugal force due to curvature will lead to significant radial pressure gradient in the flow core region [18]. In the proximity of curved ducts inner and outer walls, however, the axial velocity and the centrifugal force will approach zero. Hence, to balance the momentum transport, secondary flows will appear. This is indeed the case, as can be seen in fig. 3, where the secondary flow with higher velocities is generated in the outer wall of spiral ducts. On closer inspection, it is observed that the higher secondary flow velocity up to around 10 ms^{-1} is somewhat obtained by rectangular 4×1; meanwhile, trapezoid cross-section has the lowest secondary velocity. This can be adequately explained by the fact that at the same flow rate, smaller cross-section area drive higher amount of mass flux which lead to a higher velocity. It is further expected that the presence of secondary flow will lead to an enhancement on convection heat transfer, as will be shown later.
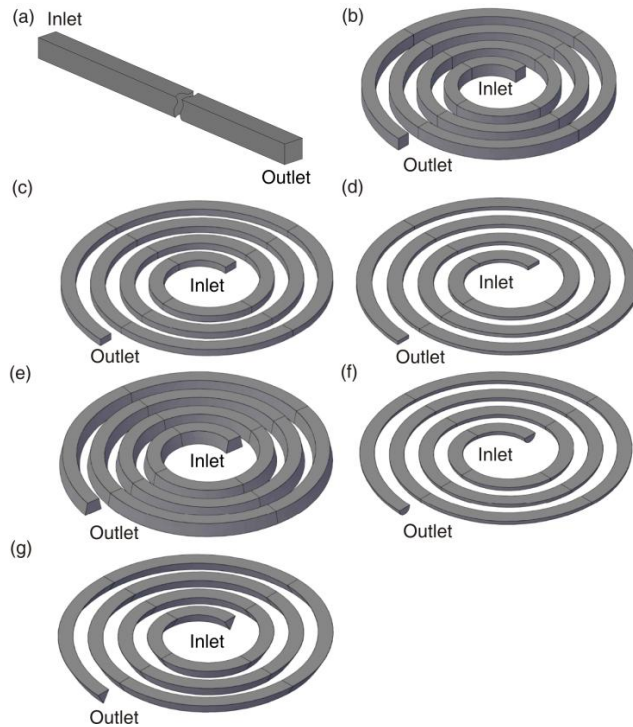

Figure 2. Computational domain for (a) straight duct and in-plane spiral with (b) square, (c) rectangular 2×1, (d) rectangular 4×1, (e) trapezoid, (f) half circular, and (g) triangular cross-sections

Table 2. Operating parameters

Parameters	Value	Unit
$\dot{m}_{in}$ (air)	$1.84 \cdot 10^{-4}$	kgs^{-1}
$\dot{m}_{in}$ (water)	$9.03 \cdot 10^{-3}$	kgs^{-1}
T_{in}	25	°C
T_w	50	°C
Q_w (air)	88.3	Wm^{-2}
Q_w (water)	7359.8	Wm^{-2}
P_{out} (gauge)	0	Pa

Figure 4 depicts the predicted temperature distribution for various cross-section areas at constant wall temperature. As expected, the presence of secondary flow affects the heat transfer performance; it is mirrored by a lower temperature at the outer wall. For constant wall temperature boundary condition, a lower temperature gradient means that more heat is dissipated which is mirrored by a higher heat transfer rate. Moreover, the higher intensity of the secondary flow will tend to lead to higher heat transfer rate as can be inferred from figs. 3 and 5(b) for in-plane spiral with rectangular 4×1 cross-sections.
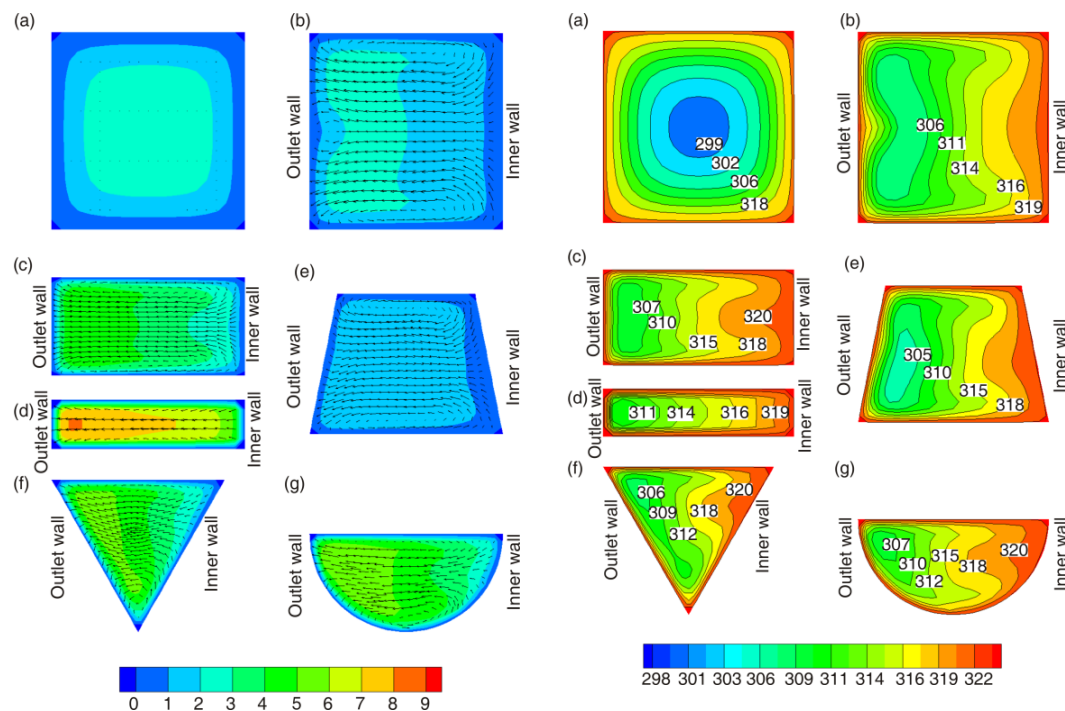

Figure 3. Axial velocity profile of air flow in (a) straight duct and in-plane spiral with (b) square, (c) rectangular 2×1, (d) rectangular 4×1, (e) trapezoid, (f) half circular, and (g) triangular cross-sections with constant wall temperature at $L = 8$ cm (color image see on our web site)

Figure 4. Temperature distribution of air flow in (a) straight duct and in-plane spiral with (b) square, (c) rectangular 2×1, (d) rectangular 4×1, (e) trapezoid, (f) half circular, and (g) triangular cross-sections with constant wall temperature at $L = 8$ cm (color image see on our web site)

Looking further into the mixed mean temperature variation along the duct length for both constant wall temperature and constant heat flux, it can be seen that the in-plane spiral ducts with trapezoid cross-section gives the highest performance while the straight duct gives the lowest heat transfer performance, as can be inferred from fig. 5. This heat transfer enhancement originates from the presence of the secondary flows at the outer wall. Similarly, for the constant heat flux case, see fig. 5(a), the trapezoid cross-section provides the best heat transfer performance compared to other configurations.
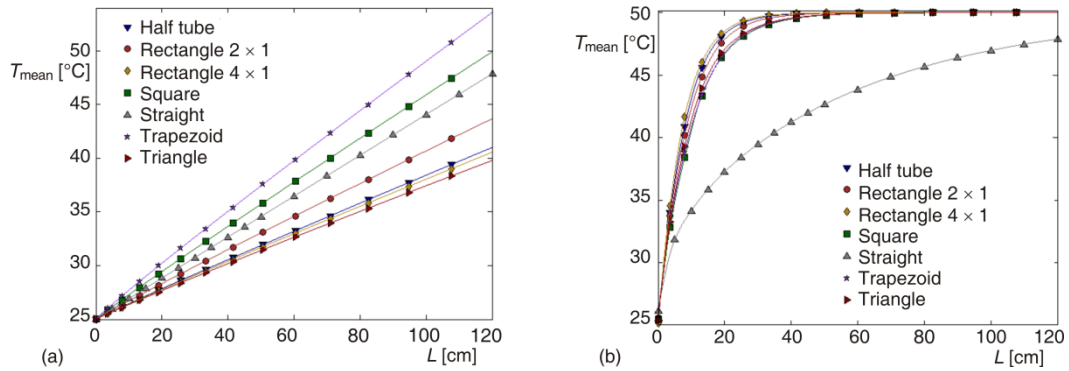
Figure 5. Mixed mean temperature of air flow for: (a) constant heat flux and (b) constant wall temperature

Another important finding is that even though in-plane spiral ducts with rectangular, triangular and half circular cross-section perform better than straight duct in constant wall temperature condition, they have lower heat transfer rate in constant heat flux condition. It indicates that the operating/boundary conditions are important factors in designing in-plane spiral ducts in heat transfer applications. For example, in a constant heat flux condition, *e. g.*, wall heated by an electrical heater, it is better to use in-plane spiral with trapezoid or square cross-section compare to straight channel; however, it is not recommended to use in-plane spiral with rectangular, half-duct, and triangular cross-section as the heat transfer is lower compare to straight duct. In contrast, for constant wall temperature applications, such as steam condenser, it is an advantageous to use in-plane spiral duct rather than using straight duct since the performance is higher for in-plane spiral ducts with all cross-sections considered here, especially with rectangular 4×1 cross-section.

With respect to heat transfer performance, it is of interest to study the effect of the Prandtl number which is represented by the fluid type (water and air). A total of 28 cases were simulated to represent various combinations of the Prandtl number and duct designs. A summary of heat transfer performance for various cases is shown in fig. 6. Here, several features are apparent; foremost is that the in-plane spiral with trapezoid cross-section yield the best heat transfer performance among others for constant wall heat flux case for both water and air; whereas for constant wall temperature, there is no significant difference for the heat
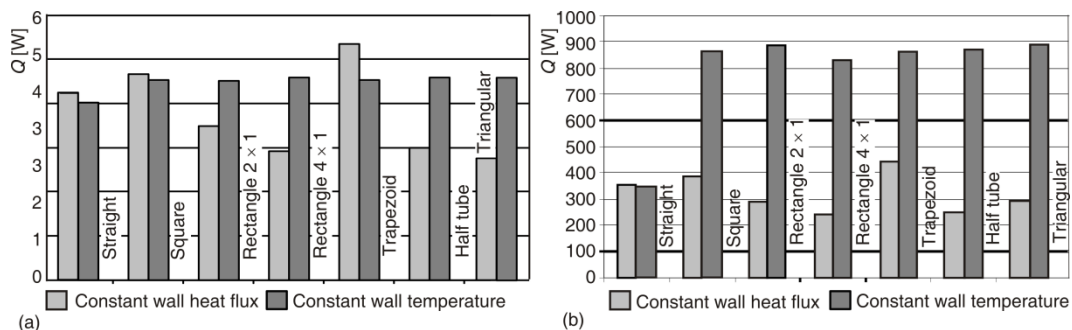

Figure 6. Total heat transfer rate [Q] of straight duct and in-plane spiral duct with various cross-sections for (a) air and (b) water

116

Kurnia, J. C., *et al.*: Laminar Convective Heat Transfer for In-Plane Spiral Coils of …
THERMAL SCIENCE, Year 2012, Vol. 16, No. 1, pp. 109-118

transfer performance for in-plane spiral with various cross-sections. In addition, it is observed that straight duct has the lowest heat transfer performance compared to in-plane spiral ducts for constant wall temperature.

A further point of interest in this study is the pumping power required to drive the flow which is mirrored by the pressure drop in the ducts – note that in this study, constant mass flow rates are fixed for all geometries. As discussed previously, the in-plane spiral with trapezoidal and rectangular cross-section give better heat transfer performance for constant heat flux and constant temperature, respectively. For rectangular 4×1 cross-section, however, the pressure drop required is the highest among others tested (up to two orders of magnitude higher than that of straight duct), as illustrated in fig. 7; the enhancement in heat transfer has to be paid by an increase in pressure drop/pumping power. A plausible explanation for the higher pressure drop is that the centrifugal force requires higher energy to overcome friction along the duct with smaller cross-section area and to generate the secondary flows. Conversely, for trapezoid cross-section, the pressure drop required to drive the flow is of the same order-of-magnitude (slightly higher) to the straight cross-section. The lower pressure drop required together with higher heat transfer performance gives advantageous for in-plane spiral with trapezoidal cross-section to be used in heat transfer applications such as heat exchanger, thermal storage, coolant plates and other applications.
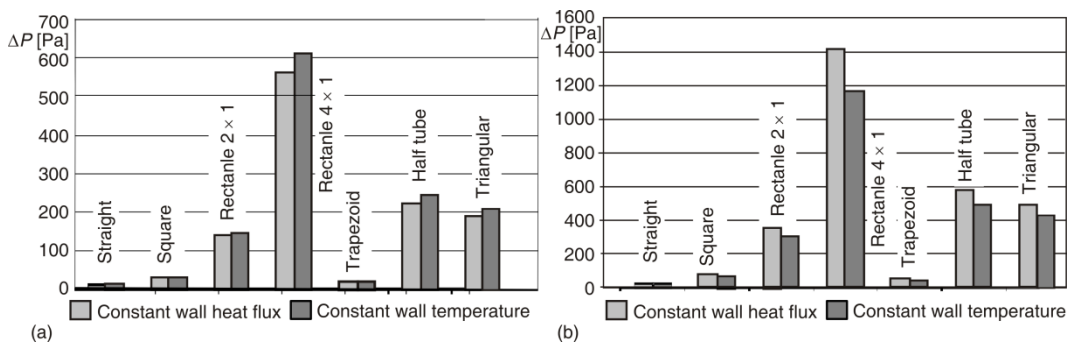

Figure 7. Pressure drop of straight duct and in-plane spiral duct with various cross-sections for (a) air and (b) water

To examine heat transfer performance the various geometries of ducts, the figure of merit concept is introduced to account the effectiveness of heat transfer performance over pressure drop. Figure 8 shows the figures of merit for various geometries. It is found that the in-plane spiral with trapezoidal cross-section has the highest figures of merit compared to others; however, it is slightly lower than that of the straight duct, except for case with water and constant wall temperature in which the figure of merit for trapezoidal is higher than straight duct, see fig. 8(b). On closer inspection, it is noted that rectangular 4×1 duct has the lowest figure of merit, followed by half-circular, triangular, rectangular 2×1 and square cross-section due to their higher pressure drop.

When designing coiled heat exchangers, however, careful balance and consideration has to be taken between compactness/size, performance, pumping power and type of applications (constant wall temperature or constant wall heat flux). If the compactness, pumping power, and performance is of interest, one can consider in-plane spiral with trapezoid cross-section to be used for various heat transfer application; for example, electrical

Kurnia, J. C., *et al.*: Laminar Convective Heat Transfer for In-Plane Spiral Coils of …
THERMAL SCIENCE, Year 2012, Vol. 16, No. 1, pp. 109-118

117

heater/stove, electronic cooling and compact heat exchanger. We have not considered the fabrication costs here.
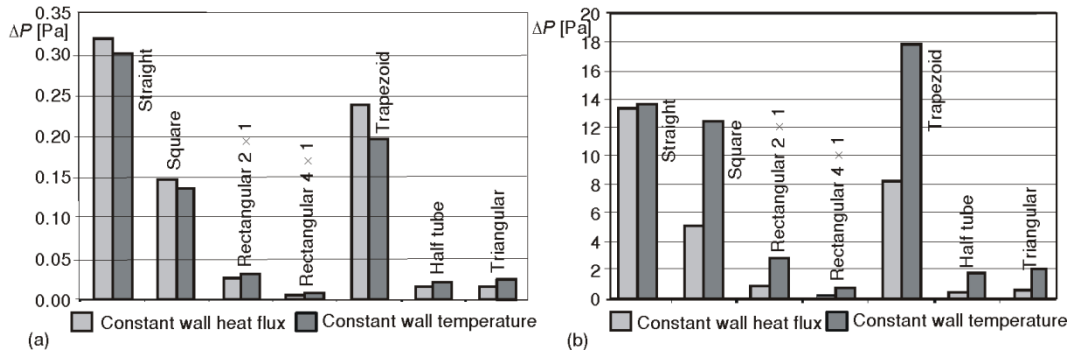

Figure 8. Figure of merit of straight duct and in-plane spiral duct with various cross-sections for (a) air and (b) water

Conclusions

A computational study was conducted to investigate the heat transfer performance of in-plane spiral ducts with various cross-section areas. In total, six duct cross-sections – square, rectangular 2 × 1, rectangular 4 × 1, trapezoidal, half-circular, and triangular cross-section – were investigated and their performance compared with a straight duct in terms of the figure of merit. The results indicate that, on average, in-plane spiral ducts give higher heat transfer rate. However, it should be noted that for constant heat flux conditions, the heat transfer rate of in-plane spiral with rectangular, triangular and half circular cross-sections are lower than those of straight duct. They also impose significantly higher pressure drop penalty compared to the straight duct. Hence, careful consideration of the operating conditions is important in selecting the geometry of in-plane spiral duct for heat transfer application. An extension study will be conducted to examine heat transfer performance of in-plane spiral duct for electronic cooling applications.

Nomenclature

A_c – cross-section area [m^2]
c_p – specific heat capacity of gas mixture, [Jkg^{-1}K^{-1}]
$\vec{e}_x, \vec{e}_y, \vec{e}_z$ – co-ordinate of vectors $\vec{n}$
F_{merit} – figure of merit
h – height, [m]
m – mass flow rate, [kgs^{-1}]
P – pressure, [Pa]
ΔP – pressure drop, [Pa]
p – coil pith, [m]
Q – total heat transfer, [W]
R – radius of coil, [m]
s – spacing, [m]
T – temperature, [°C]
$\vec{u}$, u, v, w – velocities, [ms^{-1}]
V – mean velocity, [ms^{-1}]

w – width, [m]
x, y, z – co-ordinates, [m]

Greeks symbols

μ – dynamic viscosity, [kgm^{-1}s^{-1}]
ρ – density, [kgm^{-3}]

Subscripts

b – bottom
c – coil
i – inner
in – inlet
L – length
o – outer

p – in-plane   z – trapezoid
t – top   1 – rectangular 2×1
w – wall   2 – rectangular 4×1

References

[1] Egner, M. W., Burmeister L. C., Heat Transfer for Laminar Flow in Spiral Ducts of Rectangular Cross Section, *ASME J. Heat Transfer., 127* (2005), 3, pp. 352-356
[2] Dean, W. R., Note on the Motion of Fluid in a Curved Pipe, *Philos. Mag., 4* (1927), 20, pp. 208-223
[3] Dean, W. R., The Stream-Line Motion of Fluid in a Curved Pipe, *Philos. Mag., 5* (1927), 7, pp. 208-223
[4] Naphon, P., Suwagrai, J., Effect of Curvature Ratios on the Heat Transfer and Flow Developments in the Horizontal Spirally Coiled Tubes, *Int. J. Heat Mass Transfer, 50* (2007), 3-4, pp. 444-451
[5] Saravanan, K., Rajavel, R., An Experimental Investigation of Heat Transfer Coefficients for Spiral Plate Heat Exchanger, *Modern Appl. Sci., 2* (2008), 5, pp. 14-20
[6] Ramachandran, S., Kalaichelvi, P., Sundaram, S., Heat Transfer in a Spiral Plate Heat Exchanger for Water-Palm Oil Two Phase Systems, *Braz. J. Chem. Eng., 25* (2008), 3, pp. 483-490
[7] Rajavel, R., Saravanan, K., An Experimental Study of Spiral Plate Heat Exchanger for Electrolyte. *J. Univ. Chem. Tech. Metal., 43* (2008), 2, pp. 255-260
[8] Balakrishnan, R., Santhappan, J. S., Dhasan, M. L., Heat Transfer Correlation for a Refrigerant Mixture in a Vertical Helical Coil Evaporator, *Thermal Science, 13* (2009), 4, pp. 197-206
[9] Rajavel, R., Saravanan, K., Heat Transfer Studies on Spiral Plate Heat Exchanger, *Thermal Science, 12* (2008), 3, pp. 85-90
[10] Vijayan, R., Srinivasan, P., Experimental Evaluation of Internal Heat Exchanger Influence on R-22 Window Air Conditioner Retrofitted with R-407C, *Thermal Science, 14* (2010), 1, pp. 85-90
[11] Nakayama, A., Kokubo, N., Ishida, T., Kuwahara, F., Conjugate Numerical Model for Cooling a Fluid Flowing through a Spiral Coil Immersed in a Chilled Water Container, *Numer. Heat Transfer, Part A, 37* (2000), 2, pp. 155-165
[12] Naphon, P., Wongwises, S., An Experimental Study on the In-Tube Heat Transfer Coefficient in a Spiral Coil Heat Exchanger, *Int. Commun. Heat Mass Transfer, 29* (2002), 6, pp. 797-809
[13] Ho, J. C., Wijeysundera, N. E., An Unmixed-Air Flow Model of a Spiral Cooling Dehumidifying Unit, *Appl. Therm. Eng., 19* (1999), 8, pp. 865-883
[14] Alammar, K. N., Turbulent Flow and Heat Transfer Characteristics in u-Tubes: a Numerical Study, *Thermal Science, 13* (2009), 4, pp. 175-181
[15] Kurnia, J. C., Sasmito, A. P., Mujumdar, A. S., Evaluation of the Heat Transfer Performance of Helical Coils of Non-Circular Tubes, *J. Zhejiang Univ-Sci. A* (*Appl. Phys. & Eng.*), *12* (2011), 1, pp. 63-70
[16] Kurnia, J. C., Sasmito, A. P., Mujumdar, A. S., Numerical Investigation of Laminar Heat Transfer Performance of Various Cooling Channel Design, *Appl. Therm. Eng., 31* (2011), 6-7, 1293-1304
[17] Kays, W., Crawford, M., Weigand, B., Convective Heat and Mass Transport, 4th ed., MacGraw Hill, Singapore, 2005
[18] Vashisth, S., Kumar, V., Nigam, K. D. P., A Review on the Potential Applications of Curved Geometries in Process Industry, *Ind. Eng. Chem. Res., 47* (2008), 10, 3291-3337